

DOI:10.1002/ejic.201300537

A Silicon-Heteroaromatic System as Photosensitizer for Light-Driven Hydrogen Production by Hydrogenase Mimics

Roman Goy,^[a] Ulf-Peter Apfel,^[b] Catherine Elleouet,^[c]
Daniel Escudero,^[d] Martin Elstner,^[a] Helmar Görls,^[a]
Jean Talarmin,^{*[c]} Philippe Schollhammer,^[c] Leticia González,^{*[e]}
and Wolfgang Weigand^{*[a]}

Dedicated to Professor Wolfgang Beck

Keywords: Photocatalysis / Enzyme models / Iron / Sulfur / Silicon / Hydrogenase

The utilization of light and inexpensive catalysts to afford hydrogen represents a huge challenge. Following our interest in silicon-containing [FeFe]-hydrogenase ([FeFe]-H₂ase) mimics, we report a new model approach for a photocatalytic [FeFe]-H₂ase mimic **1**, which contains a 1-silafluorene unit as a photosensitizer. Thereby, the photoactive ligand is linked to

the [2Fe2S] cluster through S-CH₂-Si bridges. Photochemical H₂ evolution experiments were performed and revealed a turnover number (TON) of 29. This is the highest reported photocatalytic efficiency for an [FeFe]-H₂ase model complex in which the photosensitizer is covalently linked to the catalytic center.

Introduction

The conversion of light into a storable energy source is a highly desired endeavor. In particular, the photocatalytic reduction of water into hydrogen affords an ideal fuel, which is easy to store in large quantities.^[1–3] In addition, the combustion of hydrogen to water has a high specific energy value (142 MJ kg⁻¹)^[4] and affords no polluting emissions.^[5]

Hydrogen is part of the biological cycle and appears as a biological energy source and transporter.^[6] Numerous structurally modified and photocatalytically functionalized models have been inspired by the structure of [FeFe]-hydro-

genase ([FeFe]-H₂ase). Multicomponent systems containing a surplus of ruthenium photosensitizers or organic fluorophores and [2Fe2S] clusters were investigated and showed moderate H₂ development upon irradiation with light.^[7–11] Multiple covalently linked dyads were synthesized with porphyrin or ruthenium units as the photosensitizer.^[12–18] These complexes revealed low turnover numbers (TON < 0.15) for H₂ generation.^[12–18] To the best of our knowledge, there is only one system containing a ruthenium photosensitizer covalently connected to the [2Fe2S] cluster by an azadithiolato linker and it showed significant H₂ development with a turnover number of 11.8.^[19] Furthermore, supramolecular assemblies comprising [2Fe2S] model compounds with an InP nanophotocathode,^[20] ZnS nanoparticles,^[21] multichromophoric hexad self-assemblies,^[22] or Mn₂Ru complexes^[23] as light-harvesting molecules were reported. Also, micellar systems^[24] and dendrimer-based mimics^[25] were utilized to allow for photocatalytic H₂ development in aqueous media.

However, water splitting by utilizing light and inexpensive catalysts to afford hydrogen still represents a huge challenge, as most complexes show a lack of reactivity and stability.^[26–31]

In continuation of our research on silicon-containing [FeFe]-H₂ase mimics,^[32–34] we aimed to synthesize a small, compact, heavy-metal-free, and easily accessible photocatalytic [FeFe] model complex (Scheme 1) by utilizing a silicon-

[a] Institut für Anorganische und Analytische Chemie, Friedrich-Schiller-Universität, Humboldtstraße 8, 07743 Jena, Germany
Fax: +49-3641-948102
E-mail: wolfgang.weigand@uni-jena.de
Homepage: http://www.uni-jena.de/Prof_W_Weigand.html

[b] Institut für Anorganische Chemie, Ruhr-Universität Bochum, Universitätsstraße 150, 44780 Bochum, Germany

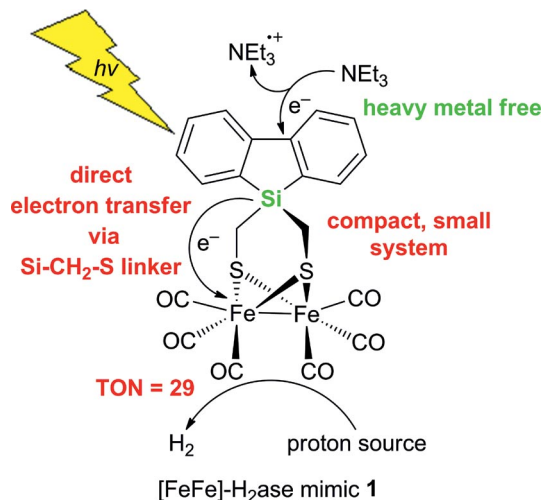
[c] Chimie, Electrochimie Moléculaires et Chimie Analytique, Université de Bretagne Occidentale, 6 Avenue Victor le Gorgeu, CS93837, 29238 Brest cedex 3, France

[d] Max-Planck-Institut für Kohlenforschung, Kaiser-Wilhelm-Platz 1, 45470 Mülheim an der Ruhr, Germany

[e] Institut für Theoretische Chemie, Universität Wien, Währinger Str. 17, 1090 Wien, Austria

Supporting information for this article is available on the WWW under <http://dx.doi.org/10.1002/ejic.201300537>.

containing heteroaromatic system. Silicon-containing aromatics are well known for their good optical properties such as light-emission and absorption in the longer wavelength area or their electroluminescence properties^[35–41] as well as for their interesting physical properties.^[42–46]



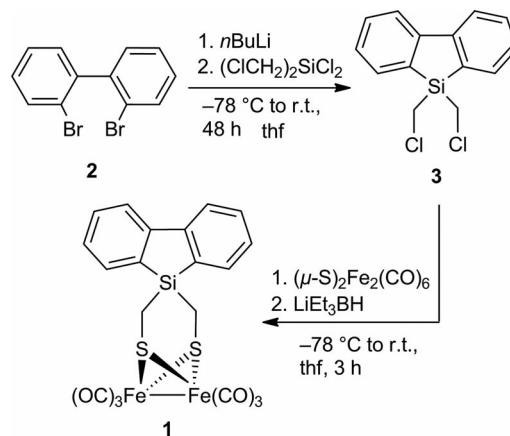
Scheme 1. Schematic representation of the light-driven production of hydrogen by [FeFe]-H₂ase mimic **1**.

Herein, we present a new model approach for a photocatalytic [FeFe]-H₂ase mimic **1**, which contains 1-silafluorene as a photosensitizer. Thereby, the photoactive ligand is linked to the [2Fe2S] cluster through S–CH₂–Si bridges, and the photoactive 1-silafluorene is directly connected with the redox-active iron center (Scheme 1).

Results and Discussion

The 1-silafluorene complex **1** was prepared according to Scheme 2. The reaction of 2,2'-dibromobiphenyl (**2**), *n*-butyllithium, and bis(chloromethyl)dichlorosilane afforded 1,1'-bis(chloromethyl)-1-silafluorene (**3**) as a colorless oil in 70% yield. Subsequent reaction with [(μ -S)₂Fe₂(CO)₆] according to known procedures gave [FeFe]-H₂ase mimic **1** as a red-brown solid in 32% yield and it was characterized by ¹H and ¹³C{¹H} NMR spectroscopy, IR spectroscopy, and mass spectrometry.^[47]

The molecular structure of **1** (Figure 1, crystal data in Table 1) shows the characteristic [2Fe2S] butterfly core. The Si atom is surrounded in a distorted tetrahedral fashion. Notably, all of the C–Si–C angles [92.2(2)–114.2(3)°] differ significantly from those of an ideal tetrahedron. Additionally, both Si–C–S angles [123.3(3) and 122.9(3)°] are best explained by sp² rather than sp³ hybridization. Similar observations were recently reported for other [2Fe2S(Si)] complexes.^[32] Additionally, Glass and co-workers reported a related [2Fe2S(Sn)] complex.^[48] Consistent with our observations, enhanced S–C–Sn angles were observed and an interaction between a σ (Sn–C) orbital and a 3p(S) orbital was verified by photoelectron spectroscopy.^[48] We assume that the large angle (170.54°) between the planes generated by C1–Si1–C2 and S1–C1C2–S2 is an indicator for an effective



Scheme 2. Reaction pathway towards **1**.

photoelectron transfer between the photosensitizer and the diiron center. A comparable orbital interaction between the σ (Si–C) orbital and a 3p(S) orbital in **1** is, therefore, very likely. A similar interaction is not reported for [Fe₂(CO)₆-(pdt)] (pdt = propanedithiolate), which shows an angle between the C–C–C and S–CC–S planes of 137.09°.^[49] Cyclic voltammetry (CV) experiments at slow-to-moderate scan rates (0.05 ≤ ν ≤ 1 V s⁻¹) show that the electrochemical re-

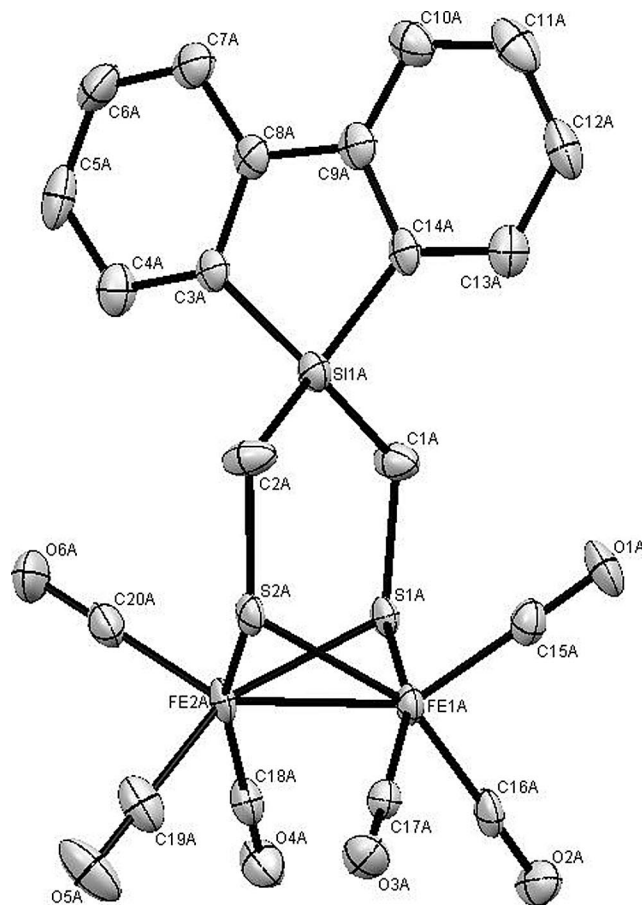


Figure 1. ORTEP view of **1** (ellipsoids at the 50% probability level).

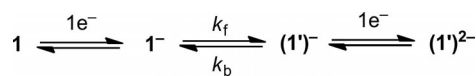
duction of $[\text{Fe}_2(\text{CO})_6\{\mu\text{-SCH}_2\text{Si}(\text{R})\text{CH}_2\text{S}\}]$ (**1**) at $E_{1/2} = -1.55$ V is quasireversible in $\text{CH}_2\text{Cl}_2/[\text{NBu}_4][\text{PF}_6]$.^[50]

Table 1. Selected bond lengths [Å] and angles [°] for **1**.

Fe(1A)–Fe(2A)	2.5268(10)
Fe(1A)–S(1A)	2.2490(15)
Fe(1A)–S(2A)	2.2563(14)
Fe(2A)–S(1A)	2.2504(15)
Fe(2A)–S(2A)	2.2428(15)
S(1A)–C(1A)	1.817(6)
S(2A)–C(2A)	1.821(6)
C(1A)–Si(1A)	1.880(6)
C(2A)–Si(1A)	1.865(6)
Si(1A)–C(3A)	1.867(6)
Si(1A)–C(14A)	1.864(6)
C(3A)–C(8A)	1.418(8)
C(9A)–C(14A)	1.418(8)
C(8A)–C(9A)	1.481(8)
Fe(1A)–Fe(2A)–S(1A)	55.86(4)
Fe(1A)–Fe(2A)–S(2A)	55.58(4)
Fe(1A)–S(1A)–Fe(2A)	68.33(4)
Fe(1A)–S(2A)–Fe(2A)	68.34(5)
S(1A)–C(1A)–Si(1A)	123.3(3)
S(2A)–C(2A)–Si(1A)	122.9(3)
C(1A)–Si(1A)–C(2A)	112.8(3)
C(3A)–Si(1A)–C(14A)	92.2(2)
C(1A)–Si(1A)–C(3A)	112.9(3)
C(2A)–Si(1A)–C(14A)	112.7(3)
C(3A)–Si(1A)–C(2A)	114.2(3)
C(14A)–Si(1A)–C(1A)	110.5(3)

A comparison of the potentials of the reduction of **1** with those of bis(mercaptomethyl)silane $[(\text{SCH}_2)_2\text{Si}(\text{Me}_2); E_{1/2} = -1.52$ V],^[32] pdt $[\text{S}(\text{CH}_2)_3\text{S}; E_{1/2} = -1.74$ V],^[51] and benzenedithiolate (bdt: $\text{SC}_6\text{H}_4\text{S}; E_{1/2} = -1.44$ V)^[52] analogues, which were measured under similar experimental conditions, indicates that the electronic effect exerted by the Si-containing bridge of **1** is intermediate between that of the pdt and the bdt ligands. A comparison of the reduction peak current (i_p^{red}) of **1** with the oxidation peak current (i_p^{ox}) of an equimolar bis-N-heterocyclic carbene (bis-NHC) complex $[\text{Fe}_2(\text{CO})_4(\kappa^2\text{-I}_{\text{Me}}\text{-CH}_2\text{-I}_{\text{Me}})(\mu\text{-pdt})]$ ($\text{I}_{\text{Me}} = 1$ -methylimidazol-2-ylidene), which was previously shown to undergo a one-electron oxidation, demonstrates that the former involves the transfer of two electrons (Figure S1).^[53–55] The single-step two-electron transfer arises from an inversion of the potentials of the individual one-electron reduction processes, $E^\circ_2 - E^\circ_1 > 0$, as already observed for a variety of diiron hexacarbonyl complexes bearing different dithiolate bridges.^[32,52,56–60] Typically, a potential inversion is observed when a chemical reaction (most often linked to a structural change) makes the second electron transfer thermodynamically more favorable than the first.^[61–65] The structural change can either be concerned with one of the electron transfers^[32,52,56–59] or appears as the intervening step of an ECE process.^[50,60] In the present case, CV at faster scan rates ($1 \leq \nu \leq 20$ V s⁻¹) leads to a significant decrease of the current function ($i_p^{\text{red}}/\nu^{1/2}$) for the reduction of **1** (Figures S1 and S2). This strongly suggests that the abovementioned rearrangement, probably involving the cleavage of the Fe–S bond, is the intervening

reaction of an EC_{rev}E process (see Scheme 3). This result is in accordance with the observation by Evans and co-workers,^[60] and hence an EE mechanism can be discarded.



Scheme 3. Proposed EC_{rev}E mechanism.

The UV/Vis absorption spectra of **1** and **3** are shown in Figure 2 for comparison. Time-dependent density functional theory (TD-DFT) calculations have been performed (see computational details in the Supporting Information) to get an insight into the UV/Vis characteristics of **1** and **3**. The theoretical UV/Vis spectra of **1** and **3** are also shown in Figure 2, and the main electronic excited states are highlighted (for a complete description of the main electronic TD-DFT excitations see Table S1). Both compounds have intense absorption bands at 210–242 and 277–290 nm, which are theoretically attributed to $\pi\text{-}\pi^*$ excitations within the 1-silafluorene moiety (for example, see S_2 and S_4 for **3** and S_{33} and S_{56} for **1** in Figure 2 and Table S1). The UV/Vis spectra of **1** and **3** differ in the low-energy regime. Only **1** has a broad band peaking at ca. 330 nm. The states responsible for this band have $\sigma\text{-}\sigma^*$ and $d\text{-}\sigma^*$ character and involve the Fe–Fe unit (see S_4 and S_9 in Figure 2 and the orbitals involved in these excitations in Figures S5 and S6). As can be seen in Figure 2, this band is slightly energetically underestimated by the TD-DFT calculations. Obviously, the latter metal-based intense band determines the photochemical and photophysical properties of **1**. Thus, upon excitation of the brighter $\pi\text{-}\pi^*$ band, new deactivation pathways involving the $\sigma\text{-}\sigma^*/d\text{-}\sigma^*$ states (either of singlet and triplet character) arise. Hereby, the energy absorbed by the 1-silafluorene chromophore can be transferred in the course of photo-deactivation to the $[(\mu\text{-S})_2\text{Fe}_2(\text{CO})_6]$ catalytic unit. The population of low-lying $\sigma\text{-}\sigma^*/d\text{-}\sigma^*$ triplet excited states (owing to strong spin–orbit couplings for Fe) guarantees that the lifetimes of the excited states are increased, and, hence, the quenching of photoluminescence and/or the photochemical hydrogen evolution is favored. Indeed, the lowest triplet excited state is adiabatically only 0.64 eV above the singlet ground state. Furthermore, the lowest triplet excited-state geometry shows longer Fe–Fe distances (see Figure S4). Such active species are then responsible for the catalytic activity of **1**, as the longer Fe–Fe distance allows for the coordination of hydrogen at the Fe–Fe core, and ultimately the H₂ evolution in the photocatalytic center by the coordination of an additional hydrogen atom is favored. The emission spectra of **1** and **3** upon excitation of the $\pi\text{-}\pi^*$ band with an excitation wavelength of 255 nm are shown in Figure 3.

To test whether a photoinduced electron transfer (PET) occurs in this system, the spectral change in the presence of triethylamine was studied. As shown in Figure 3, the emission intensity of **3** decreases upon addition of triethylamine, and the maximum of the emission shifts from 387 to 395 nm (**3** + 150 equiv. NEt₃). The decrease of the emission intensity under these conditions is reasonable as triethyl-

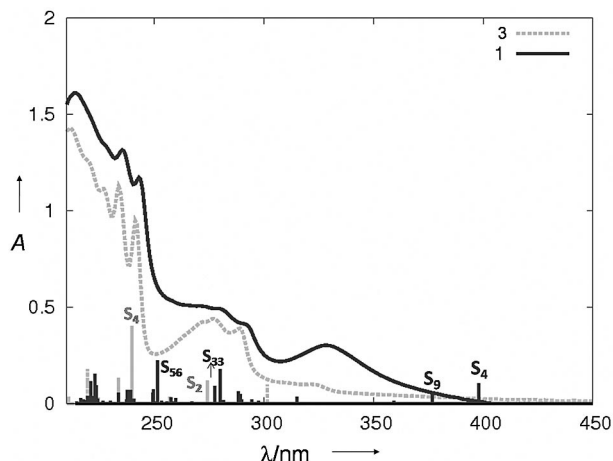


Figure 2. Experimental UV/Vis spectra for **1** and **3** (0.027 mm) in hexane superimposed on the TD-DFT vertical excitations. The main electronic states are highlighted (see Table S1 for assignments).

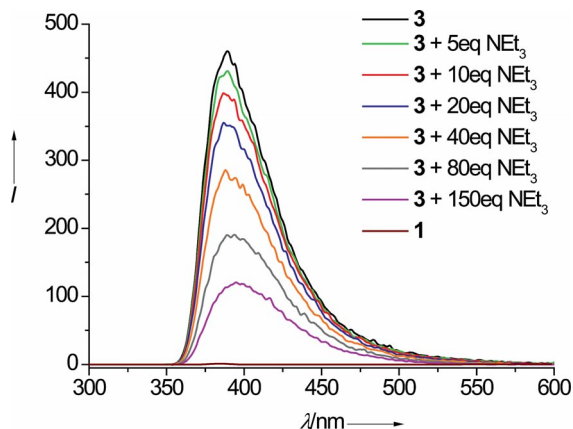


Figure 3. Photoluminescence spectra of **1** (0.27 mm) and **3** (0.092 mm) in acetonitrile in the presence of triethylamine (excitation wavelength 255 nm, $K_{SV} = 80.0 \pm 2.2 \text{ L mol}^{-1}$, see Figure S7).

amine acts as sacrificial electron donor to fill the hole generated in the π orbital upon photoexcitation. The progressive addition of NEt_3 to the solution of **3** quenched the luminescence with a rate constant K_{SV} of $80.0 \pm 2.2 \text{ L mol}^{-1}$ (Figure S7). Excitation at the characteristic absorption of both compounds at 255 nm results in a maximal luminescence at 387 nm with a quantum yield of ≤ 0.0003 for **1** and 0.183 ± 0.003 for **3** based on a 0.01 mM pyrene solution (in cyclohexane) as the reference.^[66]

Photochemical H_2 evolution experiments were performed by irradiating **1** (0.6 μmol) in the presence of trifluoroacetic acid (TFA, 1 mmol) and triethylamine (1 mmol) in acetonitrile at 254 nm with a 15 W mercury-vapor lamp. Although our experimental set up did not allow us to excite at the absorbance maximum (240 nm), we were able to obtain 17.4 μmol H_2 in the headspace of our reactor after 13 hours irradiation with our system. No further H_2 generation was observed after 13 hours. This amount of H_2 reflects a turnover number (TON) of 29 and a turnover frequency (TOF) of 2.2 h^{-1} (Figure 4) and is the

highest reported photocatalytic efficiency for an [FeFe]- H_2ase model complex in which the photosensitizer is covalently linked to the catalytic center. Headspace analysis of a mixture of **1**, Et_3N , and TFA stored in the dark revealed only traces of H_2 and further supports the necessity to photoexcite the complex to achieve catalytic activity. To further substantiate the importance of **1** for the photocatalytic hydrogen generation, an acetonitrile solution containing TFA (1 mmol) and Et_3N (1 mmol) was irradiated (254 nm) for 15 hours in the absence and presence of **3**. In both experiments, no significant generation of H_2 was observed. As reported for $\text{Fe}_3(\text{CO})_{12}$ and $\text{Fe}_2(\text{CO})_9$, irradiation with UV light in the presence of a photosensitizer can lead to significant CO dissociation and finally to the decomposition of the catalyst.^[70,71]

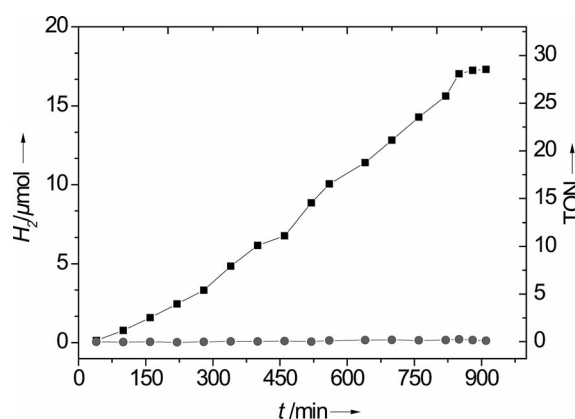


Figure 4. Light-driven hydrogen production by **1** (0.6 μmol , 0.15 mm) in the presence of trifluoroacetic acid (1 mmol, 0.25 M) and triethylamine (1 mmol, 0.25 M) in degassed acetonitrile at 25 °C. H_2 was detected by gas chromatography. Black line: with **1**, grey line: no catalyst.

To test the stability of our system, a solution of **1** was irradiated under the conditions described above and the UV/Vis spectra were recorded (Figures S8 and S9). In the absence of TFA and Et_3N , a new band at 295 nm with a stronger absorbance was observed and overlapped with the band at 330 nm. Further photoexcitation of the solution for a prolonged period of time resulted in stronger absorbance intensities for all bands and a redshift of 30 nm for the band initially observed at ca. 230 nm. After 3 h, a third band was growing in at 340 nm. Additionally, irradiation of the mixture for 15 h resulted in the loss of the characteristic CO resonances in the ^{13}C NMR spectrum of **1**, which indicates dissociation of the CO ligand. This process was further confirmed by IR spectroscopy, which showed no remaining CO bands. These observations indicate that in the absence of a sacrificial electron donor and proton source, irradiation of the complex results in CO dissociation, which finally deactivates the complex for the photocatalytic H_2 generation. Even though catalytic activity was still observed after 13 hours, experiments in the absence of Et_3N and TFA suggested decomposition of **1** after 7.5 hours. Thus, we assume that different PET quenching mechanisms under the catalysis conditions are likely.

To test this hypothesis, we repeated the irradiation experiment in the presence of TFA and Et₃N. The UV/Vis spectrum showed different spectroscopic features than the UV/Vis spectrum of the mixture without sacrificial electron donors and acid. This observation suggests a different reaction pattern in the presence of TFA and Et₃N, which is most likely because of a PET quenching processes (Figure S9). A significant redshift was observed for the band at 250–270 nm. Furthermore, in contrast to the experiments without TFA and Et₃N, the intensity of this band increases considerably faster and visibly results in higher extinction coefficients. After 240 min, a new band at 283 nm with a strong absorbance was observed. An additional band at 295 nm was observed and shifts to 315 nm upon excitation. Contrary to our experiments in the absence of TFA and NEt₃, no band at 340 nm was observed, which further confirms a different reaction pathway.

Conclusions

With the synthesis of **1**, we provide a viable synthetic pathway towards the first photocatalytic model complex of the [FeFe]-H₂ase active site with the photosensitizer directly imbedded into the bridging dithiolate unit. Thus, the photosensitizer is in close proximity to the catalytic [2Fe2S] cluster and allows for an effective electron transfer. In comparison to the influence of phosphanes,^[67] cyanides^[68] or NHCs,^[69] the implementation of the photosensitizer into the bridge revealed only moderate influence on the [2Fe2S] cluster; thus, the fluorophore can be changed without alteration of the mechanism of H₂ formation. The Si–C–S angles from the X-ray-structure are in accordance with sp² hybridization of the carbon atom; therefore, a “filled–filled” interaction between the σ(Si–C) orbital and the 3p(S) orbital is favored and, hence, there is direct communication between the photosensitizer and the [2Fe2S] cluster. This behavior was also investigated by DFT calculations and confirmed by the photocatalytic H₂ evolution with the highest reported TON for such a small [FeFe]-H₂ase model complex. Even though photocatalytic systems with higher turnover numbers exist, the elimination of Ir, Pt, Rh, or Re complexes as photosensitizers makes this design a powerful platform for the further development of proton reduction catalysts. However, a precise statement about the nature of the different intermediates during the photocatalytic hydrogen generation cannot be given, and further investigations to discover the mechanism for the H₂ development with **1**, possible degradation pathways, and visible-light-driven catalysis with the presented core structure are currently in progress. This will allow the properties of this platform to be tuned to achieve, for example, excitation with visible light and higher turnover numbers.

Experimental Section

General Procedures: All reactions were performed under a dry nitrogen or argon atmosphere with standard Schlenk techniques. All

solvents were dried and distilled according to standard methods prior to use. Et₃BHLi (1.0 M in THF), 1,2-dibromobenzene, and bis(chloromethyl)dichlorosilane are commercially available and were used without further treatment.

Infrared spectra were measured with a Bruker IFS 66 spectrometer (resolution ± 4 cm⁻¹) with the samples dispersed in compressed KBr pellets. Preparative column chromatography was performed with silica gel (Fluka, Kieselgel 60). UV/Vis spectra were recorded with a Specord S600 spectrometer, and fluorescence spectra were recorded with a Perkin–Elmer LS50B spectrometer. ¹H, ¹³C, and ²⁹Si NMR spectra were obtained with either a BRUKER Avance 200 or Avance 400 spectrometer. Elemental analyses were performed with a Vario EL III CHNS analyzer from Elementar Analysensysteme GmbH. Mass spectra were measured with a FINNIGAN MAT SSQ710 instrument.

Structure Determination: Single crystals suitable for X-ray analysis were mounted on a fiber loop and placed in a cold, gaseous nitrogen stream on a Nonius KappaCCD diffractometer performing ϕ and ω scans at 120(2) K. Diffraction intensities were measured by using graphite-monochromated Mo-*K*_α radiation ($\lambda = 0.71073$ Å). Data were corrected for Lorentz and polarization effects, but not for absorption.^[72,73] The structure was solved by direct methods (SHELXS) and refined by full-matrix least-squares techniques against *F*_o² (SHELXL-97).^[74] All hydrogen atoms were included at calculated positions with fixed thermal parameters. All non-hydrogen atoms were refined anisotropically.^[74]

CCDC-905950 contains the supplementary crystallographic data for this paper. These data can be obtained free of charge from The Cambridge Crystallographic Data Centre via www.ccdc.cam.ac.uk/data_request/cif.

Crystallographic Data of 1: C₂₀H₁₂Fe₂O₆S₂Si, *M*_r = 552.21 g mol⁻¹, red-brown prism, size 0.06 × 0.06 × 0.05 mm, monoclinic, space group *P*2₁/*c*, *a* = 13.8679(3), *b* = 26.8618(7), *c* = 11.6998(3) Å, β = 92.863(1)°, *V* = 4352.93(18) Å³, *T* = -140 °C, *Z* = 8, ρ_{calcd} = 1.685 g cm⁻³, $\lambda(\text{Mo-}K_{\alpha}) = 0.71073$ Å, $\mu(\text{Mo-}K_{\alpha}) = 16.15$ cm⁻¹, *F*(000) = 2224, 26452 reflections in *h*(-18/17), *k*(-34/33), *l*(-15/15), measured in the range 2.11° ≤ θ ≤ 27.50°, completeness $\theta_{\text{max}} = 98.9\%$, 9877 independent reflections, *R*_{int} = 0.0915, 8063 reflections with *F*_o > 4σ(*F*_o), 559 parameters, 0 restraints, *R*_{1,obs} = 0.0756, *wR*_{2,obs} = 0.1849, *R*_{1,all} = 0.0939, *wR*_{2,all} = 0.1977, Goodness-of-fit on *F*² = 1.149, largest difference peak and hole: 1.265/−1.016 e Å⁻³.

Electrochemical Procedures: The electrochemical experiments were conducted under an inert atmosphere of nitrogen or argon. The preparation and purification of the supporting electrolyte ([NBu₄][PF₆]) was performed as described previously.^[75] Trifluoromethanesulfonic acid (Aldrich) was used as received. Cyclic voltammetry was performed in a three-electrode cell by using a radiometer potentiostat (PGSTAT 128N or μ-Autolab III) driven by the GPES software. The working electrode consisted of a vitreous carbon disk, which was polished on a felt tissue with alumina, thoroughly rinsed with water, and dried before each CV scan. The Ag/Ag⁺ reference electrode was separated from the analyte by a CH₂Cl₂–[NBu₄][PF₆] bridge. All the potentials are reported against the ferrocene–ferrocenium couple; ferrocene was added as an internal standard at the end of the experiments.

Procedure for Photocatalytic H₂ Evolution: Photochemical hydrogen evolution experiments were performed by irradiating an acetonitrile solution of **1** in the presence of trifluoroacetic acid (TFA) and triethylamine at 254 nm with a 15 W mercury-vapor lamp in a quartz glass precision cell at room temperature. Prior to irradiation, the solution was sealed with a septum cap, degassed, and flushed

with dry nitrogen. Hydrogen was detected by gas chromatography by using a calibrated Varian CP-3800 Gas Chromatograph with a thermal conductivity detector and argon as the carrier gas.

Dibromobiphenyl (2):^[76] A solution of 1,2-dibromobenzene (21.5 g, 91.1 mmol) dissolved in THF (120 mL) was cooled to $-78\text{ }^{\circ}\text{C}$, and *n*-butyllithium (31.4 mL, 50.24 mmol, 1.6 M in hexane) was added dropwise over a period of 30 min. Within 24 h the reaction mixture was warmed to room temperature and then hydrolyzed at $0\text{ }^{\circ}\text{C}$ by using hydrogen chloride (100 mL, 0.5 M in water). The reaction mixture was extracted with diethyl ether ($4 \times 50\text{ mL}$), and the combined organic fractions were dried with sodium sulfate. Evaporation to dryness and crystallization from ethanol afforded colorless crystals (11.1 g, 78%). $^1\text{H NMR}$ (200 MHz, CD_2Cl_2): $\delta = 7.70$ (m, 2 H, $\text{CH}_{\text{aromatic}}$), 7.45–7.24 (m, 6 H, $\text{CH}_{\text{aromatic}}$) ppm. $^{13}\text{C NMR}$ (50 MHz, CDCl_3): $\delta = 142.09$ (C_q), 132.59, 130.96, 129.38, 127.1 ($\text{CH}_{\text{aromatic}}$), 123.52 (CBr) ppm. MS (DEI): $m/z = 312$ [M^+], 232 [$\text{M} - \text{Br}^+$], 152 [$\text{M} - 2\text{Br}^+$], 76 [$\text{M} - \text{C}_6\text{H}_4\text{Br}_2^+$].

Bis(chloromethyl)-1-silafluorene (3): A solution of 2,2'-dibromobiphenyl (2.0 g, 6.4 mmol) in Et_2O (25 mL) was cooled to $-78\text{ }^{\circ}\text{C}$, and *n*BuLi (1.6 M in hexane, 8.2 mL, 13 mmol) was added. The reaction solution was warmed to room temperature by removing the cooling bath and subsequent stirring overnight. The resulting solution was cooled to $-78\text{ }^{\circ}\text{C}$, and a solution of $\text{Cl}_2\text{Si}(\text{CH}_2\text{Cl})_2$ (1.5 g, 7.6 mmol) in Et_2O (5 mL) was added dropwise. The reaction mixture was stirred at $-78\text{ }^{\circ}\text{C}$ for 4 h and at room temperature for an additional 12 h. The mixture was filtered, and the solvents were evaporated by vacuum transfer under an argon atmosphere. The residue was purified by bulb-to-bulb distillation (130 $^{\circ}\text{C}/0.11\text{ mbar}$) to afford **3** as colorless oil (1.24 g, 70%). $^1\text{H NMR}$ (200 MHz, CDCl_3): $\delta = 7.85$ (t, $J = 7.6\text{ Hz}$, 2 H, $\text{CH}_{\text{aromatic}}$), 7.55 (t, $J = 7.6\text{ Hz}$, 2 H, $\text{CH}_{\text{aromatic}}$), 7.34 (m, 4 H, $\text{CH}_{\text{aromatic}}$), 3.29 (s, 4 H, CH_2) ppm. $^{13}\text{C NMR}$ (50 MHz, CDCl_3): $\delta = 148.52$ (C_q), 134.34 (CH), 131.78 (CH), 131.72 (CSi), 128.06 (CH), 121.15 (CH), 25.29 (CH_2) ppm. $^{29}\text{Si NMR}$ (79.5 MHz, CDCl_3): $\delta = -6.07$ ppm. MS (DEI): $m/z = 278$ [M^+], 229 [$\text{M} - \text{CH}_2\text{Cl}^+$], 193 [$\text{M} - \text{CH}_2\text{Cl}_2^+$], 179 [$\text{M} - (\text{CH}_2\text{Cl})_2^+$], 152 [$\text{M} - \text{Si}(\text{CH}_2\text{Cl})_2^+$]. $\text{C}_{14}\text{H}_{12}\text{Cl}_2\text{Si}$ (279.24): calcd. C 60.22, H 4.33, Cl 25.39; found C 60.27, H 4.41, Cl 25.10. IR $\tilde{\nu} = 3062$ (m), 2995 (m), 2933 (m), 2872 (m), 1963 (w), 1928 (w), 1894 (w), 1854 (w), 1820 (w), 1593 (vs), 1483 (m), 1459 (s), 1431 (s), 1384 (s), 1260 (s), 1128 (vs), 1095 (s), 786 (vs), 749 (s) cm^{-1} . UV/Vis (hexane): λ_{max} ($\log \epsilon$) = 211.7 (4.72), 233.6 (4.62), 241.2 (4.54), 277.3 (4.21), 289 (4.16), 321.7 (3.56) nm. Emission (hexane): $\lambda_{\text{max}} = 386\text{ nm}$.

[(C₁₄H₁₂SiS₂)Fe₂(CO)₆] (1): A solution of $[(\mu\text{-S})_2\text{Fe}_2(\text{CO})_6]$ (62 mg, 0.18 mmol) in THF (10 mL) was cooled to $-78\text{ }^{\circ}\text{C}$, and Et_3BHLi (0.36 mL, 0.36 mmol) was added dropwise. The solution was stirred for 15 min, and 1,1'-bis(chloromethyl)-1-silafluorene (50 mg, 0.18 mmol) was added. The mixture was warmed to room temperature and stirred at this temperature for 16 h. The volatiles were removed under vacuum, and the residue was purified by column chromatography (silica gel) with hexane as eluent. From the major red band, **1** was obtained as a red-brown solid (0.031 g, 32%). $^1\text{H NMR}$ (200 MHz, CDCl_3): $\delta = 7.81$ –7.11 (m, 8 H, $\text{CH}_{\text{aromatic}}$), 1.89 (s, 4 H, CH_2) ppm. $^{13}\text{C NMR}$ (50 MHz, CDCl_3): $\delta = 205.47$ (CO), 145.89 (C_q), 133.21 (CSi), 131.39 (CH), 129.85 (CH), 126.41 (CH), 119.16 (CH), 0.23 (SiCH_2S) ppm. MS (DEI): $m/z = 552$ [M^+], 496 [$\text{M} - \text{Fe}^+$], 468 [$\text{M} - \text{Fe}(\text{CO})^+$], 440 [$\text{M} - \text{Fe}(\text{CO})_2^+$], 412 [$\text{M} - \text{Fe}(\text{CO})_3^+$], 384 [$\text{M} - \text{Fe}(\text{CO})_4^+$], 356 [$\text{M} - \text{Fe}(\text{CO})_5^+$]. $\text{C}_{20}\text{H}_{12}\text{Fe}_2\text{O}_6\text{S}_2\text{Si}$ (552.21): calcd. C 43.50, H 2.19, S 11.61; found C 43.62, H 2.21, S 11.47. IR $\tilde{\nu} = 3069$ (w), 2925 (m), 2854 (w), 2073 (vs), 2032 (vs), 2001 (vs), 1984 (vs), 1719 (w), 1628 (w), 1594 (w), 1459 (w), 1432 (w), 1260 (w), 1132 (w), 782 (m), 750 (m) cm^{-1} .

UV/Vis (hexane): λ_{max} ($\log \epsilon$) = 213.4 (4.77), 235.3 (4.69), 242.8 (4.64), 273.9 (4.27), 288.2 (4.19), 328.4 (4.05).

Supporting Information (see footnote on the first page of this article): Electrochemical investigations, computational details, TD-DFT results, emission quenching of **3**, and irradiation of **1**.

Acknowledgments

Financial support for this work was provided by the Deutsche Bundesstiftung Umwelt (to R. G.) and the Studienstiftung des Deutschen Volkes as well as the Alexander-von-Humboldt foundation (to U.-P. A.). The authors thank B. Dietzek, L. Zedler, and J. Popp for discussions and K. Dubnack for experimental support.

- [1] L. Schlapbach, A. Züttel, *Nature* **2001**, *414*, 353–358.
- [2] C. L. Aardahl, S. D. Rassat, *Int. J. Hydrogen Energy* **2009**, *34*, 6676–6683.
- [3] W. Osborn, T. Markmaitree, L. L. Shaw, R. Ren, J. Hu, J. H. Kwak, Z. Yang, *JOM-J. Min. Met. Mater. S.* **2009**, *61*, 45–51.
- [4] C. Koroneos, *Int. J. Hydrogen Energy* **2004**, *29*, 1443–1450.
- [5] R. Cammack, M. Frey, R. Robson (Eds.), *Hydrogen as a Fuel: Learning from Nature*, Taylor and Francis, London, **2001**.
- [6] R. K. Thauer, *Eur. J. Inorg. Chem.* **2011**, 919–921.
- [7] Y. Na, J. Pan, M. Wang, L. Sun, *Inorg. Chem.* **2007**, *46*, 3813–3815.
- [8] Y. Na, M. Wang, J. Pan, P. Zhang, B. Åkermark, L. Sun, *Inorg. Chem.* **2008**, *47*, 2805–2810.
- [9] D. Streich, Y. Astuti, M. Orlandi, L. Schwartz, R. Lomoth, L. Hammarström, S. Ott, *Chem. Eur. J.* **2010**, *16*, 60–63.
- [10] W.-N. Cao, F. Wang, H.-Y. Wang, B. Chen, K. Feng, C.-H. Tung, L.-Z. Wu, *Chem. Commun.* **2012**, *48*, 8081–8083.
- [11] X. Li, M. Wang, D. Zheng, K. Han, J. Dong, L. Sun, *Energy Environ. Sci.* **2012**, *5*, 8220–8224; T. Yu, Y. Zeng, J. Chen, Y.-Y. Li, G. Yang, Y. Li, *Angew. Chem. Int. Ed.* **2013**, *52*, 5631–5635.
- [12] S. Ott, M. Kritikos, B. Åkermark, L. Sun, *Angew. Chem.* **2003**, *115*, 3407; *Angew. Chem. Int. Ed.* **2003**, *42*, 3285–3288.
- [13] L.-C. Song, M.-Y. Tang, F.-H. Su, Q.-M. Hu, *Angew. Chem.* **2006**, *118*, 1148; *Angew. Chem. Int. Ed.* **2006**, *45*, 1130–1133.
- [14] J. Ekström, M. Abrahamsson, C. Olson, J. Bergquist, F. B. Kaynak, L. Eriksson, L. Sun, H.-C. Becker, B. Åkermark, L. Hammarström, S. Ott, *Dalton Trans.* **2006**, 4599–4606.
- [15] W.-G. Wang, F. Wang, H.-Y. Wang, G. Si, C.-H. Tung, L.-Z. Wu, *Chem. Asian J.* **2010**, *5*, 1796–1803.
- [16] A. P. S. Samuel, D. T. Co, C. L. Stern, M. R. Wasielewski, *J. Am. Chem. Soc.* **2010**, *132*, 8813–8815.
- [17] X. Li, M. Wang, S. Zhang, J. Pan, Y. Na, J. Liu, B. Åkermark, L. Sun, *J. Phys. Chem. B* **2008**, *112*, 8198–8202.
- [18] A. M. Kluwer, R. Kapre, F. Hartl, M. Lutz, A. L. Spek, A. M. Brouwer, P. W. N. M. van Leeuwen, J. N. H. Reek, *Proc. Natl. Acad. Sci. USA* **2009**, *106*, 10460–10465.
- [19] J. Liu, W. Jiang, *Dalton Trans.* **2012**, *41*, 9700–9707.
- [20] T. Nann, S. K. Ibrahim, P.-M. Woi, S. Xu, J. Ziegler, C. J. Pickert, *Angew. Chem.* **2010**, *122*, 1618; *Angew. Chem. Int. Ed.* **2010**, *49*, 1574–1577.
- [21] F. Wen, X. Wang, L. Huang, G. Ma, J. Yang, C. Li, *ChemSusChem* **2012**, *5*, 849–853.
- [22] D. Gust, T. A. Moore, A. L. Moore, *Acc. Chem. Res.* **2009**, *42*, 1890–1898.
- [23] A. Magnuson, M. Anderlund, O. Johansson, P. Lindblad, R. Lomoth, T. Polivka, S. Ott, K. Stensjö, S. Styring, V. Sundström, L. Hammarström, *Acc. Chem. Res.* **2009**, *42*, 1899–1909.
- [24] H.-Y. Wang, W.-G. Wang, G. Si, F. Wang, C.-H. Tung, L.-Z. Wu, *Langmuir* **2010**, *26*, 9766–9771.
- [25] T. Yu, Y. Zeng, J. Chen, Y.-Y. Li, G. Yang, Y. Li, *Angew. Chem. Int. Ed.* **2013**, *52*, 1–6.

- [26] W. Lubitz, E. J. Reijerse, J. Messinger, *Energy Environ. Sci.* **2008**, *1*, 15–31.
- [27] M. Wang, L. Chen, X. Li, L. Sun, *Dalton Trans.* **2011**, *40*, 12793–12800.
- [28] a) M. Wang, Y. Na, M. Gorlov, L. Sun, *Dalton Trans.* **2009**, 6458–6467; b) R. Lomoth, S. Ott, *Dalton Trans.* **2009**, 9952–9959.
- [29] M. Wang, L. Sun, *ChemSusChem* **2010**, *3*, 551–554.
- [30] L. Sun, B. Akermark, S. Ott, *Coord. Chem. Rev.* **2005**, *249*, 1653–1663.
- [31] A. J. Esswein, D. G. Nocera, *Chem. Rev.* **2007**, *107*, 4022–4047.
- [32] U.-P. Apfel, D. Troegel, Y. Halpin, S. Tschierlei, U. Uhlemann, H. Görls, M. Schmitt, J. Popp, P. Dunne, M. Venkatesan, M. Coey, M. Rudolph, J. G. Vos, R. Tacke, W. Weigand, *Inorg. Chem.* **2010**, *49*, 10117–10132.
- [33] U.-P. Apfel, Y. Halpin, H. Görls, J. G. Vos, W. Wolfgang, *Eur. J. Inorg. Chem.* **2011**, 581–588.
- [34] U.-P. Apfel, H. Görls, G. A. N. Felton, D. H. Evans, R. S. Glass, D. L. Lichtenberger, W. Weigand, *Helv. Chim. Acta* **2012**, *95*, 2168–2175.
- [35] B. Z. Tang, X. Zhan, G. Yu, P. P. S. Lee, Y. Liu, D. Zhu, *J. Mater. Chem.* **2001**, *11*, 2974–2978.
- [36] T. Matsuda, S. Kadowaki, T. Goya, M. Murakami, *Org. Lett.* **2007**, *9*, 133–136.
- [37] S. Yamaguchi, K. Tamao, *Chem. Lett.* **2005**, *34*, 2–7.
- [38] M. Hissler, *Coord. Chem. Rev.* **2003**, *244*, 1–44.
- [39] S. Yamaguchi, C. Xu, T. Okamoto, *Pure Appl. Chem.* **2006**, *78*, 721–730.
- [40] G. Yu, S. Yin, Y. Liu, J. Chen, X. Xu, X. Sun, D. Ma, X. Zhan, Q. Peng, Z. Shuai, B. Tang, D. Zhu, W. Fang, Y. Luo, *J. Am. Chem. Soc.* **2005**, *127*, 6335–6346.
- [41] K. Tamao, *J. Organomet. Chem.* **2000**, *611*, 5–11.
- [42] S. Grigoras, *Synth. Met.* **1992**, *49*, 293–304.
- [43] G. Frapper, M. Kertesz, *Organometallics* **1992**, *11*, 3178–3184.
- [44] J. Kurti, P. Surjan, M. Kertesz, G. Frapper, *Synth. Met.* **1993**, *57*, 4338–4343.
- [45] Y. Yamaguchi, J. Shioya, *Mol. Eng.* **1993**, *2*, 339–347.
- [46] Y. Yamaguchi, *Mol. Eng.* **1994**, *3*, 311–320.
- [47] L.-C. Song, C.-G. Li, J. Gao, B.-S. Yin, X. Luo, X.-G. Zhang, H.-L. Bao, Q.-M. Hu, *Inorg. Chem.* **2008**, *47*, 4545–4553.
- [48] R. S. Glass, N. E. Gruhn, E. Lorange, M. S. Singh, N. Y. T. Stessman, U. I. Zakai, *Inorg. Chem.* **2005**, *44*, 5728–5737.
- [49] E. J. Lyon, I. P. Georgakaki, J. H. Reibenspies, M. Y. Darensbourg, *Angew. Chem.* **1999**, *111*, 3373; *Angew. Chem. Int. Ed.* **1999**, *38*, 3178–3180.
- [50] The parameters i_p and E_p are the peak current and the peak potential of a redox process, respectively; $E_{1/2} = (E_p^a + E_p^c)/2$; E_p^a and E_p^c are the potentials of the anodic and cathodic peaks of a reversible process; v (Vs^{-1}) is the scan rate in CV experiments. An ECE process is a chemical reaction (C) between two electron transfer steps (E).
- [51] K. Charreteur, M. Kdider, J.-F. Capon, F. Gloaguen, F. Y. Pétilion, P. Schollhammer, J. Talarmin, *Inorg. Chem.* **2010**, *49*, 2496–2501.
- [52] J.-F. Capon, F. Gloaguen, P. Schollhammer, J. Talarmin, *J. Electroanal. Chem.* **2004**, *566*, 241–247.
- [53] D. Morvan, J.-F. Capon, F. Gloaguen, A. Le Goff, M. Marchivie, F. Michaud, P. Schollhammer, J. Talarmin, J.-J. Yaouanc, R. Pichon, N. Kervarec, *Organometallics* **2007**, *26*, 2042–2052.
- [54] D. Chouffai, G. Zampella, J.-F. Capon, L. De Gioia, A. Le Goff, F. Y. Pétilion, P. Schollhammer, J. Talarmin, *Organometallics* **2012**, *31*, 1082–1091.
- [55] We made the reasonable assumption that the diffusion coefficient of **1** is close to that of $[Fe_2(CO)_4(\kappa^2-I_{Me}-CH_2-I_{Me})(\mu-pdt)]$.
- [56] G. A. N. Felton, A. K. Vannucci, J. Chen, L. T. Lockett, N. Okumura, B. J. Pedro, U. I. Zakai, D. H. Evans, R. S. Glass, D. L. Lichtenberger, *J. Am. Chem. Soc.* **2007**, *129*, 12521–12530.
- [57] J. Chen, A. K. Vannucci, C. A. Mebi, N. Okomura, S. C. Borowski, M. Swenson, L. T. Lockett, D. H. Evans, R. S. Glass, D. L. Lichtenberger, *Organometallics* **2010**, *29*, 5330–5340.
- [58] J. Windhager, M. Rudolph, S. Bräutigam, H. Görls, W. Weigand, *Eur. J. Inorg. Chem.* **2007**, 2748–2760.
- [59] J.-F. Capon, S. Ezzaher, F. Gloaguen, F. Y. Pétilion, P. Schollhammer, J. Talarmin, T. Davin, J. E. McGrady, K. W. Muir, *New J. Chem.* **2007**, *31*, 2052–2064.
- [60] G. A. Felton, B. J. Petro, R. S. Glass, D. L. Lichtenberger, D. H. Evans, *J. Am. Chem. Soc.* **2009**, *131*, 11290–11291.
- [61] For leading references, see: a) D. H. Evans, *Chem. Rev.* **2008**, *108*, 2113–2144; b) W. E. Geiger, *Prog. Inorg. Chem.* **1985**, *33*, 275–352; c) D. H. Evans, K. M. O’Connell, in: *Electroanalytical Chemistry*, vol. 14 (Ed.: A. J. Bard), Dekker, New York, **1986**, p. 113–207.
- [62] D. Urhammer, F. A. Schultz, *J. Phys. Chem. A* **2002**, *106*, 11630–11636.
- [63] J. B. Fernandes, L. Q. Zhang, F. A. Schultz, *J. Electroanal. Chem.* **1991**, *297*, 145–161.
- [64] D. T. Pierce, W. E. Geiger, *J. Am. Chem. Soc.* **1992**, *114*, 6063–6073, and references cited therein.
- [65] A. J. Downard, A. M. Bond, A. J. Clayton, L. R. Hanton, D. A. McMorrin, *Inorg. Chem.* **1996**, *35*, 7684–7690.
- [66] The quantum yield of pyrene is 0.32, see: I. B. Berlman, *Handbook of Fluorescence Spectra of Aromatic Molecules*, Academic Press, New York, **1971**.
- [67] a) X. Zhao, I. P. Georgakaki, M. L. Miller, J. C. Yarbrough, M. Y. Darensbourg, *J. Am. Chem. Soc.* **2001**, *123*, 9710–9711; b) X. Zhao, I. P. Georgakaki, M. L. Miller, R. Mejia-Rodriguez, C.-Y. Chiang, M. Y. Darensbourg, *Inorg. Chem.* **2002**, *41*, 3917–3928; c) D. Chong, I. P. Georgakaki, R. Mejia-Rodriguez, J. Sanabria-Chinchilla, M. P. Soriaga, M. Y. Darensbourg, *Dalton Trans.* **2003**, *21*, 4158–4163; d) R. Mejia-Rodriguez, D. Chong, J. H. Reibenspies, M. P. Soriaga, M. Y. Darensbourg, *J. Am. Chem. Soc.* **2004**, *126*, 12004–12014.
- [68] a) F. Gloaguen, J. D. Lawrence, M. Schmidt, S. R. Wilson, T. B. Rauchfuss, *J. Am. Chem. Soc.* **2001**, *123*, 12518–12527; b) J. D. Lawrence, T. B. Rauchfuss, S. R. Wilson, *Inorg. Chem.* **2002**, *41*, 6193–6195; c) J. L. Nehring, D. M. Heinekey, *Inorg. Chem.* **2003**, *42*, 4288–4292.
- [69] J.-F. Capon, S. E. Hassnaoui, F. Gloaguen, P. Schollhammer, J. Talarmin, *Organometallics* **2005**, *24*, 2020–2022.
- [70] F. Gärtner, A. Boddien, E. Barsch, K. Fumino, S. Losse, H. Junge, D. Hollmann, A. Brückner, R. Ludwig, M. Beller, *Chem. Eur. J.* **2011**, *17*, 6425–6436.
- [71] F. Gärtner, B. Sundararaju, A.-E. Surkus, A. Boddien, B. Loges, H. Junge, P. H. Dixneuf, M. Beller, *Angew. Chem.* **2009**, *121*, 10147–10150.
- [72] COLLECT, Data Collection Software, Nonius B. V., The Netherlands, **1998**.
- [73] Z. Otwinowski, W. Minor, *Processing of X-ray Diffraction Data Collected in Oscillation Mode*, in: *Methods in Enzymology*, vol. 276: *Macromolecular Crystallography, Part A* (Eds.: C. W. Carter Jr., R. M. Sweet), Academic Press, **1997**.
- [74] G. M. Sheldrick, *Acta Crystallogr., Sect. A* **2008**, *64*, 112–122.
- [75] J.-F. Capon, F. Gloaguen, P. Schollhammer, J. Talarmin, *J. Electroanal. Chem.* **2004**, *566*, 241–247.
- [76] F. R. Leroux, L. Bonnafox, C. Heiss, F. Colobert, D. A. Lanfranchi, *Adv. Synth. Catal.* **2007**, *349*, 2705–2713.

Received: April 23, 2013
Published Online: July 4, 2013